UCRL-CONF-232503

LAWRENCE
LIVERMORE
NATIONAL
LABORATORY

Neutron-Absorbing Coatings for Safe Storage of Fissile Materials with Enhanced Shielding & Criticality Safety

J-S. Choi, J.C. Farmer, C. Lee, L. Fischer, M. Boussoufi, B. Liu, H. Egbert

July 5, 2007

Disclaimer

NEUTRON-ABSORBING COATINGS FOR SAFE STORAGE OF FISSILE MATERIALS WITH ENHANCED SHIELDING & CRITICALITY SAFETY

J-S. Choi, J. Farmer, C. Lee and L. Fischer
Lawrence Livermore National Laboratory, Livermore, California USA

M. Boussoufi, B. Liu and H. Egbert
McClellan Nuclear Radiation Center, McClellan, California USA

Abstract

Neutron-absorbing Fe-based amorphous-metal coatings have been developed that are more corrosion resistant than other criticality-control materials, including Al-B_4C composites, borated stainless steels, and Ni-Cr-Mo-Gd alloys. The presence of relatively high concentration of boron in these coatings not only enhances its neutron-absorption capability, but also enables these coatings to exist in the amorphous state.

Exceptional corrosion resistance has been achieved with these Fe-based amorphous-metal alloys through additions of chromium, molybdenum, and tungsten. The addition of rare earth elements such as yttrium has lowered the critical cooling rate of these materials, thereby rendering them more easily processed. Containers used for the storage of nuclear materials, and protected from corrosion through the application of amorphous metal coatings, would have greatly enhanced service lives, and would therefore provide greater long-term safety.

Amorphous alloy powders have been successfully produced in multi-ton quantities with gas atomization, and applied to several half-scale spent fuel storage containers and criticality control structures with the high-velocity oxy-fuel (HVOF) thermal spray process. Salt fog testing and neutron radiography of these prototypes indicates that such an approach is viable for the production of large-scale industrial-scale facilities and containers.

The use of these durable neutron-absorbing materials to coat stainless steel containers and storage racks, as well as vaults, hot-cell facilities and glove boxes could substantially reduce the risk of criticality in the event of an accident. These materials are particularly attractive for shielding applications since they are fire proof.

Additionally, layers of other cold and thermal sprayed materials that include carbon and/or carbides can be used in conjunction with the high-boron amorphous metal coatings for the purpose of moderation. For example, various carbides, including boron, tungsten, and chromium carbide, as well as graphite particles can be co-deposited with a metallic binder phase with either thermal spray or cold spray technology. These moderator layers would also be fire resistant.

By coating the vessels and piping used for spent fuel reprocessing, including slab and pencil tanks, enhanced criticality safety and substantially better corrosion resistance can be achieved simultaneously. Since these alloys are Fe-based, any substitution of these for high-performance Ni-based alloys is expected to result in a cost savings. Ultimately, the cost of these materials should comparable to that of stainless steels.

Introduction

Several Fe-based amorphous alloys have been developed with very good corrosion resistance [1-6]. Many of these alloys are based upon a common parent alloy, and can be applied as thermal spray coatings [7]. Two of the most promising formulations are SAM2X5 and SAM1651, which include chromium (Cr), molybdenum (Mo), and tungsten (W) for enhanced corrosion resistance, boron (B) to enable glass formation and neutron absorption; and yttrium (Y) to lower the critical cooling rate during the glass forming process.

SAM2X5 – $Fe_{49.7}Cr_{17.7}Mn_{1.9}Mo_{7.4}W_{1.6}B_{15.2}C_{3.8}Si_{2.4}$
SAM1651 – $Fe_{48}Cr_{15}Mo_{14}B_6C_{15}Y_2$

The capability to scale-up the thermal spray of ultra-hard corrosion-resistant coatings of SAM2X5 and SAM1651 has been demonstrated successfully during the coating of several half-scale spent nuclear fuel (SNF) containers and criticality control assemblies (baskets).

A half-scale model SNF container made of Type 316L stainless steel was coated with SAM2X5 (Lot # 06-015 powder with range of particle sizes of 53/+15 microns) by using a JK2000™ gun in a thermal spray process with high-velocity oxy-fuel (HVOF). The container was fabricated from Schedule 10 pipe, had lengths of approximately 90 inches, diameters of approximately 30 inches, and wall thicknesses of approximately 0.3712 inches. The coating was nominally 17 ± 2 mils (~ 0.5 mm) thick, with typical bond strengths of 5,000 to 10,000 pounds per square inch (5-10 ksi), porosities of less than one percent (< 1%) and extreme hardness.

The half-scale container, coated with SAM2X5, showed no corrosion after salt-fog testing (Figures 1). In contrast, the 1018 carbon steel reference samples experienced severe corrosive attack after eight abbreviated cycles in the salt-fog test (Figure 2).

Figure 1 – Half-scale Type 316L stainless steel container coated with SAM2X5 Lot # 06-015, deposited HVOF with JK2000™ gun, photographed after atmospheric salt-fog test.

Figure 2 – Corrosive attack of 1018 carbon steel reference samples during atmospheric salt-fog test.

Half-scale type 316L stainless steel criticality control assemblies (baskets) were also coated with SAM2X5 Lot # 06-015 (Figure 3). These prototypes were imaged with neutron radiography at the McClellan Nuclear Radiation Center (MNRC) TRIGA reactor.

Figure 3 – Inspecting the half-scale type 316L stainless steel criticality control assemblies (baskets) coated with SAM2X5 by Plasma Technology, Inc. (PTI). The SAM2X5 powders were produced by The Nanosteel Co. (TNC). (The picture shows from left: A. D'Amato of PTI, J. Buffa of TNC, C. Lee and J. Choi of LLNL).

The boron content and corrosion resistance of Fe-based amorphous alloys such as SAM2X5 and the flexibility of applying these alloys on metal substrates by thermal spray process render them attractive candidates for criticality control applications required for the safe long-term storage of spent nuclear fuel [8]. The average neutron transmission cross-sections of SAM2X5 and other criticality control materials, including borated stainless steel and Ni-Cr-Mo-Gd alloy, were measured at MNRC. While it has been shown in other experiment that these amorphous alloys are also more corrosion resistant than borated stainless steel and Ni-Cr-Mo-Gd [9], this paper summaries the fast neutron radiation effect on these amorphous alloys under irradiation in the MNRC TRIGA reactor; the transmission cross section measurements of these alloys; and their suitability as shielding materials in stringent fire-protection environment.

Fast Neutron Radiation Effect

Several series of SAM melt-spun ribbons were prepared for irradiation experiment in the Neutron Irradiation Facility (NIF) and in the core of the TRIGA reactor at MNRC (Figure 4 and 5).
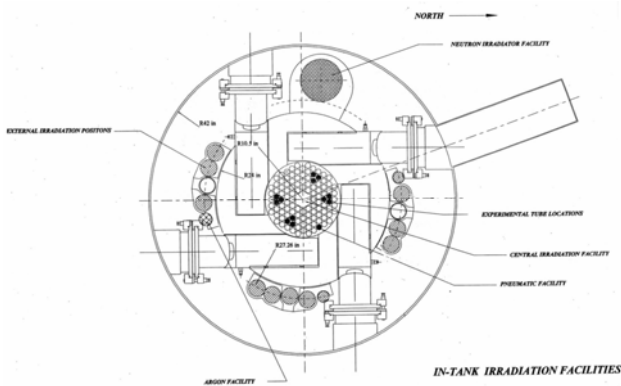
Figure 4 – MNRC Reactor Internal

Figure 5 – Outer Container for the Neutron Irradiation Facility (NIF)

Table I shows the specific ingredients of the 2 SAM series of ribbons (SAM2X and SAM3X) used in the irradiation experiment.

Table I – Two series of SAM melt-spun ribbons prepared for irradiation experiment

Mo Series DAR40* + Mo	+ 1% Mo (SAM2X1)	+ 3% Mo (SAM2X3)	+ 5% Mo (SAM2X5)	+ 7% Mo (SAM2X7)
Y Series DAR40* + Y	+ 1% Y (SAM3X1)	+ 3% Y (SAM3X3)	+ 5% Y (SAM3X5)	+ 7% Y (SAM3X7)

Note: * DAR40 – $Fe_{49.7}Cr_{17.7}Mn_{1.9}Mo_{2.4}W_{1.6}B_{15.2}C_{3.8}Si_{2.4}$

The melt-spun ribbons, after X-ray diffraction (XRD) were inserted into the NIF for three irradiation cycles. Table II shows the irradiation cycles; time of exposure in reactor; total exposure fluence (defined as the flux multiplied by time) and the equivalent time, in years of radiation exposure of material inside the spent fuel containers in the Yucca Mountain (YM) repository environment.

Table II – Two series of SAM melt-spun ribbons prepared for irradiation experiment

Irradiation cycle (fast flux = 1.5×10^{10} (n/cm2-sec)	1st	2nd	3rd
Total time exposed in reactor, min	44	132	263
Total exposure fluence, flux x time	4.3×10^{13}	1.3×10^{14}	2.6×10^{14}
Equivalent years in YM environment	~670	~2000	~4000

X-ray diffraction (XRD) was used to examine the melt-spun ribbons at each irradiation cycle and after a total cumulative time exposure of 263 minutes at a fast neutron flux of 1.5×10^{10} n/cm^2-sec. This exposure equates to a total neutron fluence of 2.6×10^{14} n/cm^2, or an equivalent time in YM environment of ~4000 years. A ten-fold increase in fluence was achieved in subsequent irradiation of these ribbons by inserting them into the central location of the reactor core.

The use of XRD is to identify the presence of crystalline phases in these ribbons. The XRD spectra of an amorphous material does not have sharp peaks; whereas, the XRD spectra of a crystalline material or a material that is a mixture of amorphous and crystalline material will have sharp peaks.

Figure 6 shows the post-irradiation XDR results of the two series of SAM melt-spun ribbons. It indicates that the extensive fast neutron irradiation does not change the structure of the amorphous SAM2X and SAM3X melt-spun ribbons.
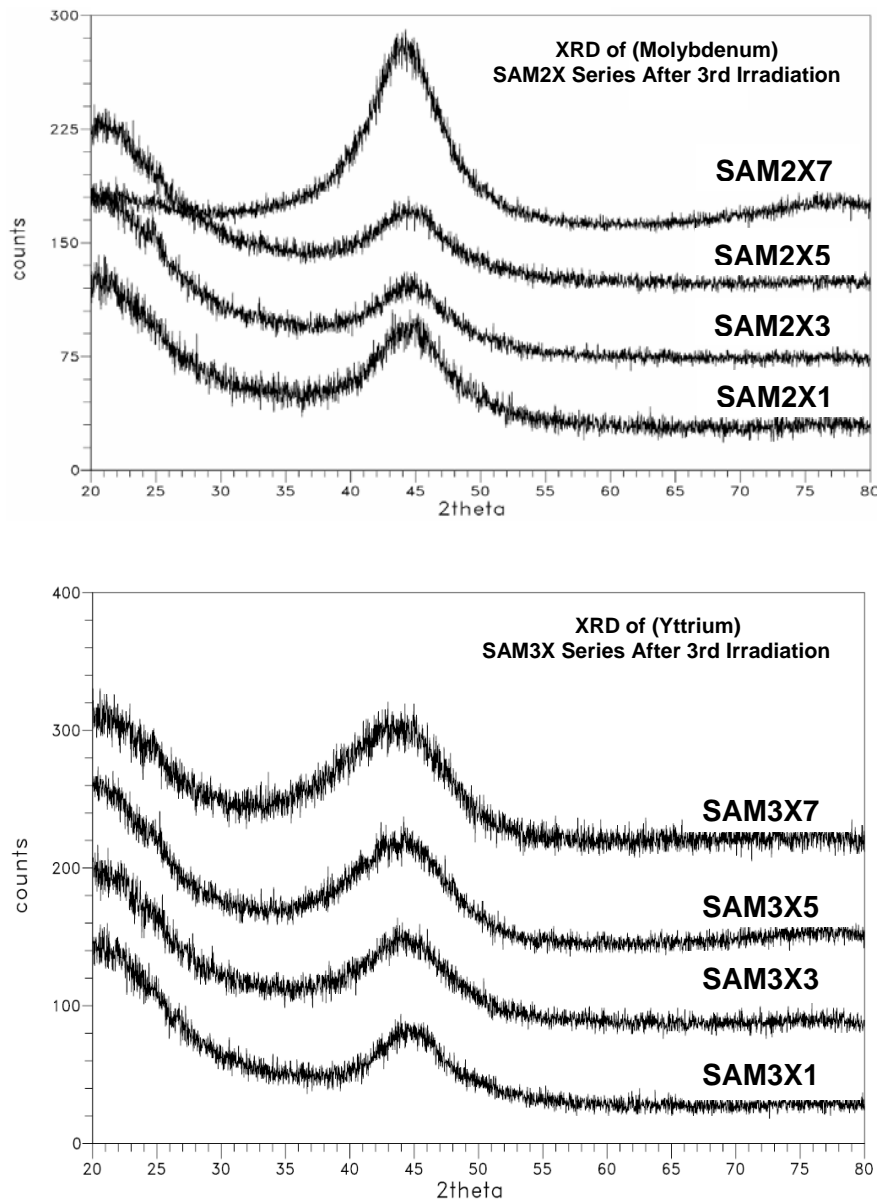

Figure 6 – XRD results of neutron irradiation of SAM ribbons.

Thermal Neutron Transmission Measurements

When thermal neutron passes through an absorbing material, it can be either absorbed, scattered away, or transmitted through. The ability of the neutron absorbing material to capture the neutron can be estimated by the transmission measurement. For strong thermal neutron absorbers (e.g., ^{157}Gd, ^{155}Gd, and ^{10}B, etc) the thermal neutron incident intensity is reduced mainly by the absorption of neutron, and minimally by the scattering effect. The transmission intensity is hence, estimated based on the following relationship:

$$I_t = I_o \, e^{(-\sigma t \, * \, n \, * \, d)}$$
$$= I_o \, e^{(-\Sigma t \, * \, d)}$$

where I_t is the thermal neutron transmission intensity
   I_o is the incident intensity of the thermal neutron
   σ is the microscopic transmission cross section
   n is the atom density of the neutron absorbing material (e.g., ^{10}B, etc.)
   d is the thickness of the neutron absorbing material
   Σ_t is the macroscopic cross section, defined as the probability per unit path length that a neutron will interact as it moves about in a medium

The mean free path, λ is defined as $1/\Sigma_t$, which is the average distance that a neutron moves between collisions.

Both the transmission and incident thermal neutron intensity can be measured by experiment. These transmission measurements were performed for various neutron absorbers including Boral^{TM}, Metamic^{TM}, Ni-Gd, borated stainless steel, and metal substrates (C-22 and Type 316L stainless steel) coated with SAM2X5. The schematic and experimental apparatus are shown in Figure 7 and 8.
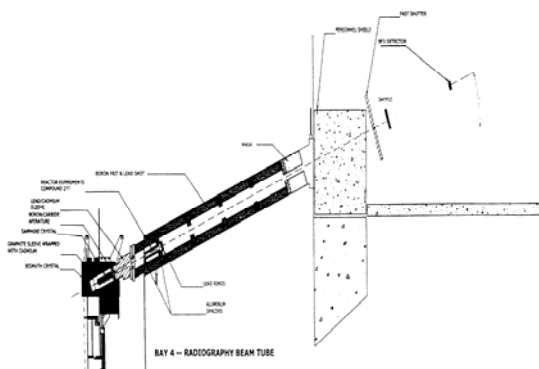

Figure 7 – Schematic of the Transmission Measurement Apparatus

Figure 8 – Transmission measurement Experiment Set-Up for a Ni-Gd Plate

Thermal neutron transmission measurements were performed at MNRC for a variety of metal plates with or without neutron absorbers. Results of transmission measurements of various neutron absorbing materials are obtained. The results are shown in Table III and compared with non-neutron absorbing substrates. It is noted that the SAM2X5 absorbs thermal neutron with an average neutron transmission cross section of about 7.1 cm^{-1}. The average Σ_t for the Ni-Gd plates from measurements is about 2.3 (and about 5.9 after adjusted for the "flux suppression" effect due to Gadolinium's large absorption cross section). The results indicate the low Σ_t for the borated stainless steel plates, due perhaps to the low boron content in these plates.

Table III – Results of transmission measurement of various neutron absorbing plates

Plate #	Plate ID	Description	Transmission Count Rate (cpm)	Bare Beam Count Rate (cpm)	Ratio	Transmission Cross Section, Σ_t, cm^{-1}
1	MNRC	Boral 40 mil or 0.1 cm thick	7550	73017	0.103	22.7
2*	316L	Base plate, 1/4" or 0.635 cm thick	39309	77478	0.507	1.07
3*	C22	Base plate, 0.28" or 0.711 cm thick	31033	77478	0.401	1.29
4*	SAM2X5 on C-22 (M18W3)	C22 1/8" or 0.317 cm thick with coating by TNC	26831	77478	0.346	6.52
5	SAM2X5 on C-22 (M10S14)	C22 1/4" or 0.635 cm thick with coating by TNC	14482	70644	0.205	7.65
6 (1)	NiGd	Labeled "Extra", 3/8" or 0.952 cm thick	1948	70644	0.0276	3.77
6 (2)	NiGd	Labeled "Extra", 3/8" or 0.952 cm thick	1897	70095	0.0271	3.79
7	Metamic	B$_4$C/ Al, 1/16" or 0.158 cm thick	4891	70644	0.0692	16.9
8	NiGd	Labeled (1), 3/8" or 0.952 cm thick	1637	67700	0.0242	3.91
9	NiGd	Labeled (2), 3/8" or 0.952 cm thick	1672	67700	0.0247	3.89
10	SAM2X5 on 316L-C1	316L 1/4" or 0.635 cm thick with coating by PTI	26037	68622	0.379	5.82
11	SAM2X5 on 316L- C2	316L 1/4" or 0.635 cm thick with coating by PTI	24875	68622	0.362	6.73
12	SAM2X5 on 316L- W1	316L 1/4" or 0.635 cm thick with coating by PTI	24026	67928	0.354	7.18
13	SAM2X5 on 316L- W2	316L 1/4" or 0.635 cm thick with coating by PTI	24263	67928	0.357	7.01
14	SAM2X5 on C22- C15	C22 1/4" or 0.635 cm thick with coating by PTI	21555	67062	0.321	6.34
15	SAM2X5 on C22- C16	C22 1/4" or 0.635 cm thick with coating by PTI	19500	67062	0.291	8.30
16	SAM2X5 on C22- W15	C22 1/4" or 0.635 cm thick with coating by PTI	19876	68606	0.290	8.37
17	SAM2X5 on	C22 1/4" or 0.635 cm thick	20857	68606	0.304	7.43

	C22- W16	with coating by PTI				
18	Borated S.S. (182193)	Borated S.S. 5/8" or 1.587 cm thick	4438	63011	0.0704	1.67
19	Borated S. S. (182194)	Borated S.S. 5/8" or 1.587 cm thick	1904	63011	0.0302	2.21
20	Borated S. S. (182196)	Borated S.S. 5/8" or 1.587 cm thick	1014	63011	0.0161	2.60
21	Borated S. S. (03180)	Borated S.S. 5/8" or 1.587 cm thick	941	63011	0.0149	2.65

Note: *Runs at 1.8 MW operating power. Other measurements were obtained when reactor was run at 1.5 MW

Criticality Analysis

A disposal container designed to hold twenty-one spent pressurized water reactor (PWR) fuel assemblies was modeled for criticality analyses. Each of the 21 Westinghouse designed 17 x 17 assembly containing 264 pins of spent UO_2 fuel, and void spaces previously occupied by 24 guide thimbles and one instrumentation tube were modeled. The PWR fuel assembly was modeled at 35 GWd/tonne of burn-up and with a 10-year decay. Several fission product isotopes (e.g., ^{149}Sm, ^{103}Rh, ^{143}Nd, ^{155}Gd, and ^{83}Kr, etc.) were also included in the evaluation model.

MCNP Version 5, a three dimensional (3-D) Monte-Carlo transport code with continuous energy groups of neutron cross-sections was used to calculate the multiplication eigenvalue (k_{eff}) of the critical configurations [10]. The criticality analyses for a disposal container model were performed. The results are shown in Table IV. Delk$_{eff}$ is the difference in k_{eff} from unity.

Table IV – Results of criticality analysis for a disposal container model.

	¼" (6.4 mm) stainless steel basket								¼" Ni-Gd basket material
	No Boron	0.12 wt. % B	1 wt. % B	2 wt. % B	No Boron 1mm SAM2X5	0.12 wt.% B & 1mm SAM2X5	No Boron 1mm SAM1651	0.12 wt. % B & 1mm SAM1651	
k_{eff}	1.00	0.96	0.90	0.88	0.92	0.91	0.95	0.94	0.93
del k_{eff}	0.0	0.04	0.10	0.12	0.08	0.09	0.05	0.06	0.07

The first set of calculations consists of borated stainless steel basket with various concentration of natural boron. It indicates that the borated stainless steel basket with 0.12 wt. % of boron would drop the k_{eff} to about 4% of that of the no boron case. The second set of calculations consists of stainless steel basket coated with 1mm of SAM2X5 and another SAM material SAM1651 (containing 1.24 wt. % boron). The stainless steel basket contains either no or 0.12 wt. % boron. The results indicate that the 1mm SAM2X5 is 2 times more effective neutron poison than the borated stainless steel with 0.12 wt. % boron. The SAM1651 has less boron, its neutron-absorbing effectiveness is comparable to the borated stainless steel.

For comparison, the k_{eff} of a Ni-Gd basket was also calculated. The Ni-Gd basket (0.635 cm thick) contains 2 wt. % gadolinium. Gadolinium is a more effective neutron

absorber than boron for low energy neutron (i.e., neutron energy < 0.025 eV). But its absorption capability drops very rapidly with higher neutron energy (starting from E > 0.1eV). The gadolinium cross sections also have a wide resonance region where the prediction of absorption capability varies widely. The calculation result for the Ni-Gd basket indicates that the neutron absorbing effectiveness of Ni-Gd is in between of the 1mm thick SAM2X5 and SAM1651.

Radiation Shielding and Fire Protection Nuclear Materials in Storage

Nuclear materials such as uranium and plutonium emit alpha particles, gamma rays, and neutron from spontaneous fission and (α, n) sources. To minimize the health-physics impact to personnel, operation of the storage facility for nuclear materials should be provided for radiation shielding. Typical shielding materials for gamma radiation are heavy-mass materials including steel, lead, and Fe-based amorphous alloys. For neutron shielding, light-mass materials such as hydrogenous material (poly-ethylene, etc.) would be preferred. However, hydrogenous materials are generally combustible and constitute to a fire hazard in storage operation.

The light-z metal alloy, Al-Li is widely used in the aircraft manufacturing industry and has good moderating characteristics for fast neutron, providing that the lithium is enriched to ^{6}Li. Partially crystalline materials such as Fe-based (Gd-B) also moderates fast neutron. Such glassy-alloy can be thermally sprayed onto structural substrate, providing high strength and possibly corrosion-resistant properties. The amorphous alloys such as SAM2X5 can be effective in neutron shielding provided that the neutron is moderated. Table V shows the comparison of shielding effectiveness of these materials while Figure 9 compares the effectiveness of neutron shielding of a plutonium metal ingot with 250 ppm ^{241}Am from 3 different materials (poly-ethylene, Al-Li, and Fe-Gd-B).

Table V – Comparison of shielding effectiveness of different materials

Material	Type	Density g/cc	Gamma Shielding	Neutron Shielding	Combustible Material
Poly-ethylene	Organic	0.95	Not good	Good	Yes
Al-Li	Metal alloy	2.5	Good	Good	No
Fe-Gd-B	Partially crystalline alloy	~7.8	Excellent	Good	No
SAM2X5	Amorphous alloy	~7.8	Excellent	Effective if neutrons are moderated	No

Figure 9 indicates that Al-Li is most effective in neutron shielding among the three (by a factor of 1.25 and 2 better than poly-ethylene and Fe-Gd-B, respectively in reducing the neutron dose rate by two orders of magnitude). While Al-Li and Fe-Gd-B are non-combustible, their higher densities, as compared to that of poly-ethylene would add weight and hence, could render them unsuitable for shielding design. In some applications, a combination of a neutron moderating material and a high-boron amorphous alloy coating could provide an effective neutron shielding with reduced fire-

loading to the storage facility. For example, various carbides, including boron, tungsten, and chromium carbide, as well as graphite particles can be co-deposited with a metallic binder phase with either thermal spray or cold spray technology. These moderator layers would also be fire resistant.
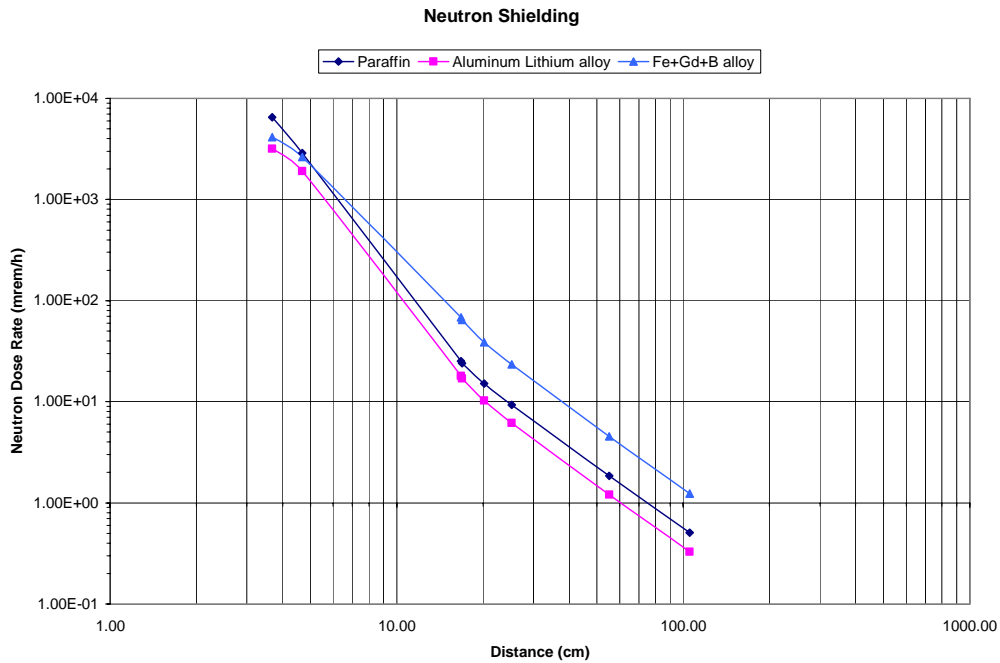
Neutron Shielding

Figure 9 – Comparison of Radiation Dose Rates for a Plutonium Metal Ingot with 250 ppm [241]Am among Parafin (poly-ethylene), aluminum-lithium, and Fe-based-(Gd-B) partially amorphous metal

Summary

1. The high boron-containing SAM2X5 coating can be an effective criticality control material for the spent fuel containers. The HVOF thermal-spray process is a demonstrated technology to apply SAM coating onto alloy substrates.
2. The neutron irradiation experiment indicates that the amorphous alloys are stable and their amorphous structures are not changed after exposure to high doses of fast neutron irradiation.
3. The neutron transmission measurements indicate that SAM2X5-costed substrates exhibit effective thermal neutron absorbing capability. The transmission cross sections of SAM2X5 coatings are three-to-four times higher than that of borated stainless steel, and twice that of the nickel-gadolinium alloy.
4. The SAM2X5-coated metallic substrate is effective in gamma shielding. It may not be as good for neutron shielding due to its dense mass and lack of neutron moderation capability. For neutron shielding in stringent fire-protection environment, other types of light-mass metal, such as Al-Li, or semi-amorphous alloys, such as Fe-Gd-B may be considered.

Acknowledgments

References

1. J. C. Farmer et al.: High-performance corrosion-resistant amorphous metals. In *Global 2003*, New Orleans, LA (American Nuclear Society, 2003).
2. J. C. Farmer, J. J. Haslam, S. D. Day, D. J. Branagan, M. C. Marshall, B. E. Mecham, E. J. Buffa, C. A. Bue, J. D. K. Rivard, D. C. Harper, M. B. Beardsley, D. T. Weaver, L. F. Aprigliano, L. Kohler, R. Bayles, E. J. Lemieux, T. M. Wolejsza, N. Yang, G. Lucadamo, J. H. Perepezko, K. Hildal, L. Kaufman, A. H. Heuere, F. Ernst, G. M. Michal, H. Kahn and E. J. Lavernia: High-performance corrosion-resistant materials, iron-based amorphous-metal thermal-spray coatings. *High-Performance Corrosion-Resistant Materials (HPCRM) Annual Report*, UCRL-TR-206717 (LLNL, Livermore, CA, September 28, 2004).
3. J. C. Farmer, J. J. Haslam, S. D. Day, D. J. Branagan, C. A. Blue, J. D. K. Rivard, L. F. Aprigliano, N. Yang, J. H. Perepezko, and M. B. Beardsley: Corrosion characterization of iron-based high-performance amorphous-metal thermal-spray coatings. In *Pressure Vessels and Piping Division Conference, Denver, CO, July 17-21, 2005*, Paper PVP2005-71664, (ASME, New York, NY, 2005).
4. J. C. Farmer, J. J. Haslam, S. D. Day, T. Lian, R. Rebak, N. Yang, and L. Aprigliano: Corrosion resistance of iron-based amorphous metal coatings. Paper PVP2006-ICPVT11-93835, In *Pressure Vessels and Piping Division Conference, Vancouver, BC, July 23-27, 2006* (ASME, New York, NY, 2006a).
5. J. Farmer, J. Haslam, S. Day, T. Lian, C. Saw, P. Hailey, J-S. Choi, N. Yang, C. Blue, W. Peter, J. Payer and D. Branagan: Corrosion resistances of iron-based amorphous metals with yttrium and tungsten additions in hot calcium chloride brine and natural Seawater, $Fe_{48}Mo_{14}Cr_{15}Y_2C_{15}B_6$ and W-containing variants. In *Critical Factors in Localized Corrosion 5, A Symposiun in Honor of Hugh Issacs*, edited by N. Missert, Electrochemical Society Transactions, Vol. 3, 210th Meeting of the ECS, Cancun, Mexico, 2006 (ECS, Pennington, NJ, 2006b).
6. J. Farmer, J. Haslam, S. Day, T. Lian, C. Saw, P. Hailey, J-S. Choi, R. Rebak, N. Yang, R. Bayles, L. Aprigliano, J. Payer, J. Perepezko, K. Hildal, E. Lavernia, L. Ajdelsztajn, D. J. Branagan, and M. B. Beardsely: A high-performance corrosion-resistant iron-based amorphous metal – the effects of composition, structure and environment on corrosion resistance. In *Scientific Basis for Nuclear Waste Management XXX*, Symposium NN, Boston, MA, November 27 to December 1, 2006 (MRS, Warrendale, PA, 2006c).

7. D. J. Branagan: U.S. Pat. 6,125,912 (2000); U.S. Pat. 6,258,185 (2001); U.S. Pat. Appl. 20030051781 (2003); U.S. Pat. Appl. 20050013723 (2004); U.S. Pat. Appl. 20040141868 (2004); U.S. Pat. Appl. 20040140021 (2004); U.S. Pat. Appl. 20040140017 (2004); U.S. Pat. 6,767,419 (2000); U.S. Pat. Appl. 20040253381 (2004); U.S. Pat. Appl. 20040250929 (2004); U.S. Pat. Appl. 20040250926, (2004).

8. J. S. Choi, J. C Farmer, C. K. Lee, "Applications of Neutron-Absorbing Amorphous Metal Coatings for Spent Nuclear Fuel (SNF) Containers: Use of Novel Coating Materials to Enhance Criticality Safety Controls," UCRL-MI-220385, Lawrence Livermore National Laboratory, Livermore, CA, June 16 (2006).

9. T. Lian, D. Day, P. Hailey, J-S. Choi, and J. Farmer: Comparative study on the corrosion resistance of Fe-based amorphous metal, borated stainless steel and Ni-Cr-Mo-Gd alloy. In *Scientific Basis for Nuclear Waste Management XXX*, Symposium NN, Boston, MA, November 27 to December 1, 2006 (MRS, Warrendale, PA, 2006).

10. MCNP5, developed by the Los Alamos National Laboratory, is a general **M**onte **C**arlo **N**-**P**article code. MCNP5 was released to ORNL/RSICC and made available to people within the US in April 2003. This release is identified as MCNP5_RSICC_1.14.